Radiation Measurements 145 (2021) 106610

Contents lists available at ScienceDirect

Radiation Measurements

journal homepage: www.elsevier.com/locate/radmeas

A model explaining the inability of exciting thermoluminescence (TL) peaks in certain low temperature ranges

J.L. Lawless [a], R. Chen [b,*], V. Pagonis [c]

[a] Redwood Scientific Incorporated, Pacifica, CA94044-4300, USA
[b] Raymond and Beverly Sackler School of Physics and Astronomy, Tel Aviv University, Tel Aviv, 69978, Israel
[c] Physics Department, McDaniel College, Westminster, MD21157, USA

ARTICLE INFO

Keywords:
Thermoluminescence
Excitation temperature
Simulations
Schön-klasens model

ABSTRACT

In some instances reported in the literature, a thermoluminescence peak that was expected to be excited by certain irradiation was not excitable at a certain temperature range below that of the peak although it was excitable at different temperature ranges. Two specific cases of this kind are calcium tungstate and semiconducting diamonds excited by UV light. The resemblance between these two different materials is quite surprising. In both cases, when the sample is UV irradiated at ~80 K and heated up, a glow curve consisting of two peaks is measured, one at ~150 K and the other at ~260 K. However, if the sample is held at temperatures between 150 and 260 K, the efficiency of excitation of the 260 K peak decreases very significantly with temperature so that it can hardly be excited above 200 K. In this work we present a possible energy-level model, previously used to explain the anomalous heating-rate effect, which can account for this rather anomalous effect. The model includes an electron trap, a hole trap and a hole recombination center. The transitions taking place during excitation, relaxation and heating are followed by using the appropriate sets of simultaneous differential equations. Simulation of the process by using a certain set of parameters is reported. Also, a theoretical account with approximations is utilized and both yield practically the same results. The effect of inability of excitation of the second peak at the temperature range between the two peaks is demonstrated.

1. Introduction

Thermoluminescence (TL) peaks are usually excitable at any temperature below that of the peak in question. Of course, the stability of a given peak depends quite strongly on the temperature at which the sample is held following excitation prior to heating, however, if heating starts rather shortly after excitation, the temperature of excitation is nearly irrelevant if it is below that of the peak. There are, however, some reports in the literature where a TL peak is not excitable at a certain temperature range well below that of the relevant peak. In two cases, namely, UV excited semiconducting diamonds and calcium tungstate, the glow curve consists of two peaks. The unusual behavior here is that in the temperature range between that of the two peaks, the higher temperature peak is not excitable. Halperin and Chen (1966) and Winer et al. (1973) (see also Chen and Pagonis (2011)) studied the UV excited TL in semiconducting diamonds. They report on two peaks following excitation at 80 K, at ~150 K and ~260 K. When the excitation was with 225 nm (5.5 eV photons), which enables the excitation of electrons across the forbidden gap, the higher-temperature peak was excitable at temperatures up to ~260 K, similar to the behavior in other materials. However, when the excitation was in the range of 300–400 nm, the peak at 260 K could not be excited at temperatures significantly above 150 K which is the temperature of the first peak. It has therefore been obvious that there is some coupling between the two peaks. Surprisingly similar results were reported by Sayer and Souder (1967, 1969) and Sayer and Lynch (1970) who had studied the UV excited TL in calcium tungstate. With UV radiation of 253.7 nm, namely 4.89 eV photons, the full glow curve is excited at 80 K. This photon energy is just sufficient to raise electrons from the valence band into the conduction band (see e.g. Mikhailik et al. (2004)). The results of the glow curve are surprisingly similar to those of semiconducting diamonds. Two peaks are observed, at ~160 K and 260 K with comparable intensity following the low-temperature excitation. However, the intensity of the 260K peak became smaller with excitation at higher temperatures, and it was not excitable at all above ~210K. As stated by Sayer and Lynch (1970), the 260 K peak could only be obtained by exciting the crystal below

* Corresponding author.
E-mail address: chenr@tau.ac.il (R. Chen).

https://doi.org/10.1016/j.radmeas.2021.106610
Received 21 March 2021; Received in revised form 11 May 2021; Accepted 4 June 2021
Available online 10 June 2021

temperatures at which the 160 K peak was also excited.

The present work offers a model which can explain a behavior very similar to that seen in calcium tungstate and semiconducting diamonds. In addition, we would like to mention some other experimental effects in other materials in which TL is not excitable in certain temperature ranges below that of the glow peak. Durrani et al. (1977) reported on the strong dependence of TL intensity in quartz on the temperature of excitation. For TL in the range of 513–693 K, the sensitivity reduced by $\sim 10^3$ as the temperature of excitation T_{irr} is reduced from room temperature to 178 K for a γ dose of 6 kGy. Kitis and Charalambous (1988, 1990) reported on the irradiation temperature dependence of some kinds of quartz and in meteorites material. For example, in material from Norton County meteorite, a peak at 380 °C could not be excited above ~500 K (227 °C). Halperin (2000) studied TL in Sawyer synthetic electron grade quartz and reported that the high temperature thermoluminescence (HTTL) in the temperature range 450–700 K could not be excited by X-irradiation below ~200 K. His explanation of this effect has to do with recombination of Li ions with Al centers. Molnár et al. (2001) reported on the influence of the irradiation temperature on TL sensitivity of Al_2O_3:C. TL sensitivity was found to decrease by ~40% with decreasing irradiation temperature between +30 and −100 °C. High temperature TL peaks were shown to appear only if the irradiation temperature was higher than 200 °C. The authors proposed a mechanism of recombination of holes with electrons in the dosimetric traps to explain these phenomena. Nikiforov et al. (2001) and Kortov et al. (2002) communicated on TL in α-Al_2O_3 excited by UV light. A peak at 450 K was found to increase significantly with the temperature of excitation with the UV exposure but was temperature independent with β irradiation.

In the present work we demonstrate that a model previously utilized to explain the possibility of getting a duplicitous TL curve and anomalous heating-rate effect, can explain the occurrence of a glow curve consisting of two peaks in which the excitation of the second peak is significantly diminished while excited in the temperature range between the two peaks. It therefore seems that there is a strong coupling between the two peaks. Thus, the results in semiconducting diamonds and calcium tungstate may be explained qualitatively. The set of parameters we chose yields in the simulation consisting of excitation, relaxation and heating a glow curve which resembles those mentioned above found in semiconducting diamonds and calcium tungstate.

2. The model

The energy-band model we use to describe this unusual effect is borrowed from a previous work (Chen et al. (2008)) which explained the possibility of a duplicitous TL curve resulting from simultaneous thermal release of electrons and holes from electron- and hole-traps. The model resembles the Schön-Klasens model (see Schön (1942); Klasens (1946)), and even more so to the model of McKeever et al. (1985), which includes an additional energy level. Note that practically the same model has been used by Chen and Pagonis (2017) for explaining the anomalous heating-rate effect in thermoluminescence as an inverse thermal quenching. The model is shown in Fig. 1. It includes an electron trapping state, N, a hole trapping state, M_2 and a hole recombination center, M_1. During excitation, the applied radiation raises electrons from the valence band to the conduction band. The free holes may get trapped at the hole trap M_2 or at the hole center M_1. At the same time, the free electron can be trapped in the electron trap, N or recombine with a hole in the center, provided that the center has trapped a hole at an earlier stage of the excitation. The addition to the previous duplicitous model, is that we allow here a recombination of free electrons with holes in the hole trap M_2, a transition denoted by the probability coefficient A_{m2}.

The set of simultaneous differential equations governing the process during excitation is

$$\frac{dn}{dt} = A(N-n)n_c - n\gamma, \tag{1}$$

$$\frac{dm_1}{dt} = B_1(M_1 - m_1)n_v - A_{m1}m_1 n_c, \tag{2}$$

$$\frac{dm_2}{dt} = B_2(M_2 - m_2)n_v - A_{m2}m_2 n_c - m_2\gamma_{m2}, \tag{3}$$

$$\frac{dn_c}{dt} = X - A(N-n)n_c - A_{m2}m_2 n_c - A_{m1}m_1 n_c + n\gamma, \tag{4}$$

$$\frac{dn_v}{dt} = X - B_1(M_1 - m_1)n_v - B_2(M_2 - m_2)n_v + m_2\gamma_{m2}. \tag{5}$$

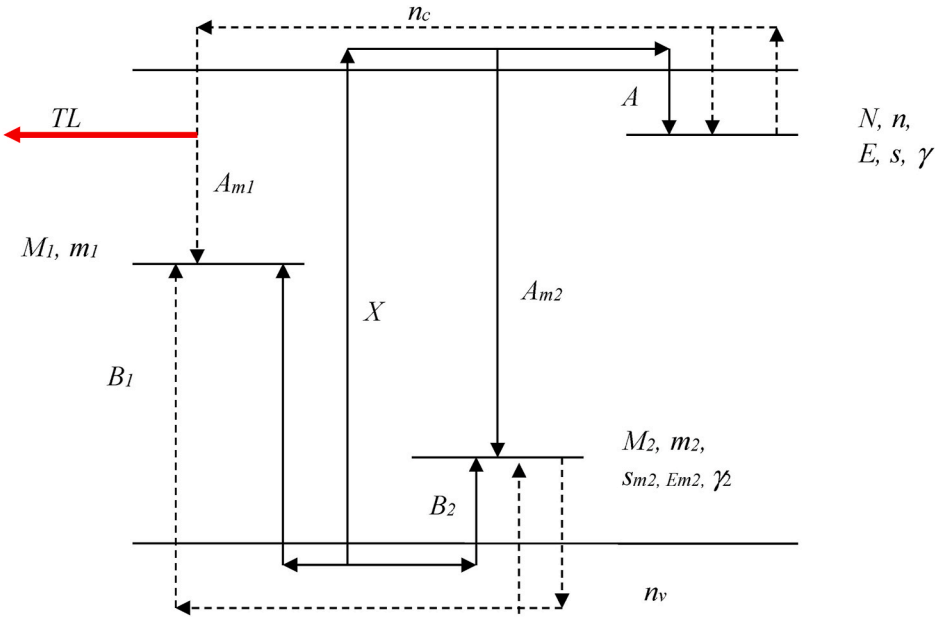

Fig. 1. Energy level diagram of the model with the relevant transitions. N is the electron trap, M_1 is the hole center and M_2 is the hole trap. The other parameters are defined in the text. Transitions taking place during excitation at low temperatures are shown in solid lines and transitions occurring at higher temperatures are given in dashed lines.

Here, N (cm^{-3}) and n (cm^{-3}) denote, respectively, the concentration and occupancy of electron traps, M_2 (cm^{-3}) and m_2 (cm^{-3}) the concentration and occupancy of hole traps and M_1 (cm^{-3}), m_1 (cm^{-3}) the concentration and occupancy of hole centers, respectively. n_c (cm^{-3}) is the instantaneous concentration of free electrons and n_v (cm^{-3}) the concentration of free holes. X ($cm^{-3}s^{-1}$) is the rate of production of electron-hole pairs by the applied radiation, proportional to the dose-rate being used. A (cm^3s^{-1}) is the trapping probability coefficient of free electrons from the conduction band into N and B_2 (cm^3s^{-1}), the trapping probability coefficient of free holes from the valence band into M_2. B_1 (cm^3s^{-1}) is the probability coefficient for free holes from the valence band to be trapped in the luminescence center, A_{m2} (cm^3s^{-1}) is the probability coefficient of electrons to fall into the hole trap M_2 and A_{m1} (cm^3s^{-1}) the probability coefficient of free electrons recombining with holes in the center. The relevant parameters for the thermal release of electrons is the activation energy E (eV) and the frequency factor s (s^{-1}), and for the release of holes, the activation energy E_{m2} (eV) and the frequency factor s_{m2} (s^{-1}); T (K) is the temperature and k (eV/K) is the Boltzmann constant. Also, we define

$$\gamma = s \exp(-E/kT), \tag{6}$$

$$\gamma_{m2} = s_{m2} \exp(-E_{m2}/kT). \tag{7}$$

3. Intuitive explanation

Let us consider the model which may explain the "disappearing" peak. We have one trap, N, one radiative center, M_1 and one non-radiative center, M_2 which also acts as a hole trap. During irradiation at $T = 100$ K, N is populated with electrons and M_1 and M_2 are populated with holes. Because the recombination coefficient of m_1 is very large in the chosen set of parameters (see below), the population of m_1 remains small compared to m_2: $m_1 << m_2$. By conservation of charge, it follows that $m_2 \approx n$.

During heating, n is the first to become thermally unstable. While many of the electrons recombine with m_2, some recombine radiatively with m_1. This yields the first peak. Because m_1 is small and its recombination coefficient large, its population is quickly depleted and light emission stops.

The trap population n continues to drop as electrons are released and recombine with m_2, but before it is completely depleted, m_2 becomes thermally unstable. When this happens, the holes from m_2 are thermally released to the valence band. Those free holes which are not retrapped by m_2 eventually become trapped in m_1. With m_1 replenished, radiative recombination starts again and we see the second peak.

The case with irradiation plus relaxation at 200 K is much simpler. Because n is thermally unstable at this temperature, the population n never grows large. If the relaxation time is long enough, it will decay

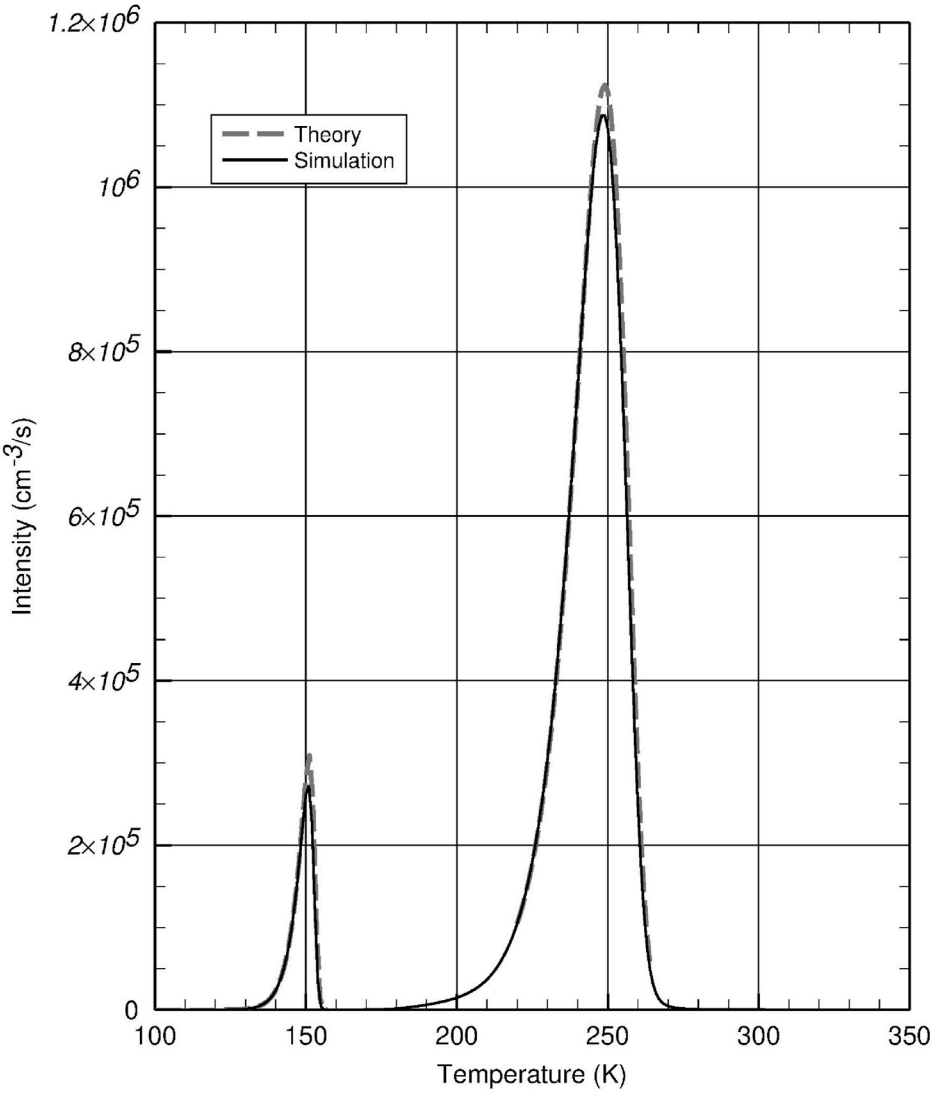

Fig. 2. The glow curve simulated by solving the equations numerically (solid line) and by the theory (dashed line).

back to zero. With a negligible population of trapped electrons, then recombination during heating is also negligible and both peaks disappear.

The model shows why there is a connection between the behavior of the two peaks as seen in semiconducting diamonds and calcium tungstate.

4. Numerical simulations and results

The solid line in Fig. 2 shows an example of a simulated glow curve based on the model. The parameters used were $N = 3 \times 10^9$ cm^{-3}; $M_2 = 10^{13}$ cm^{-3}; $M_1 = 10^{14}$ cm^{-3}; A=10^{-9} cm^{3}s^{-1}: $B_2 = 3 \times 10^{-8}$ cm^{3}s^{-1}; $B_1 = 2 \times 10^{-8}$ cm^{3}s^{-1}; $A_{m2} = 10^{-9}$ cm^{3}s^{-1}; $A_{m1} = 5 \times 10^{-6}$cm^{3}s^{-1}; $s = 5 \times 10^{12}$ s^{-1}; $s_{m2} = 3 \times 10^{12}$ s^{-1}; E=0.49 eV; $E_{m2} = 0.66$ eV; $X = 5 \times 10^7$ cm^{-3}s^{-1}. The parameters were chosen in such a way that the two TL peaks occur at ~159 K and ~260 K, similar to the peaks in semiconducting diamonds and calcium tungstate.

For this set of parameters, the simulation process was repeated for excitation temperatures between 100 K and 220 K and the maximum TL intensity of the 260 K peak found is shown in Fig. 3. As can be seen in the figure, the intensity of this peak gets smaller as the temperature of excitation increases between 150 and 220 K. The maximum intensity reduces very significantly for excitations as of ~160 K, much lower than the temperature of the peak at ~260 K.

5. Approximate analytical theory

For the conditions of our simulations, the following low-dose assumptions are well justified:

$$m_1 << M_1; \quad m_2 << M_2. \tag{8}$$

If the lifetimes of the free electrons and free holes are sufficiently short, then n_c and n_v will be small and quasi-steady approximation applies,

$$n_c = \frac{X + n\gamma}{A(N-n) + A_{m2}m_2 + A_{m1}m_1}, \tag{9}$$

$$n_v = \frac{X + m_2\gamma_{m2}}{B_1 + B_2M_2}. \tag{10}$$

In this case, the governing equations (1)–(3) reduce to

$$\frac{dn}{dt} = \frac{A(N-n)}{A(N-n) + A_{m2}m_2 + A_{m1}m_1}X - \frac{A_{m2}m_2 + A_{m1}m_1}{A(N-n) + A_{m2}m_2 + A_{m1}}n\gamma, \tag{11}$$

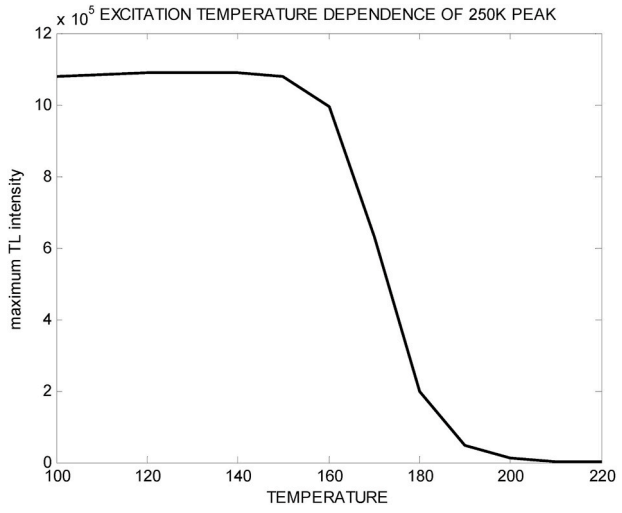

Fig. 3. The maximum intensity of the 250 K peak as a function of the excitation temperature between 100 and 220 K, as determined by the simulations.

$$\frac{dm_1}{dt} = \frac{B_1M_1}{B_1M_1 + B_2M_2}(X + m_2\gamma_{m2}) - \frac{A_{m1}m_1}{A(N-n) + A_{m2}m_2 + A_{m1}m_1}(X + N\gamma), \tag{12}$$

$$\frac{dm_2}{dt} = \frac{B_2M_2}{B_1M_1 + B_2M_2}X - \frac{A_{m2}m_2}{A(N-n) + A_{m2}m_2 + A_{m1}m_1}(X + n\gamma) - \frac{B_1M_1}{B_1M_1 + B_2M_2}m_2\gamma_{m2}. \tag{13}$$

Each of the terms in Eqs. 11–13 has clear physical meaning. For example, from Eq. (12) which conserves m_1, $(X + m_2\gamma_{m2})$ is the total rate at which free holes are created and $B_1M_1/(B_1M_1+B_2M_2)$ is the fraction of those holes that are captured by m_1.

With initial conditions n=m_1=m_2=0, charge conservation for the quasi-steady equations requires

$$n = m_1 + m_2. \tag{14}$$

For the parameters chosen, the quasi-steady approximation is valid during irradiation, relaxation and the first peak. It is not used for the second peak.

5.1. Irradiation at low temperature

For irradiation at low temperature, both n and m_2 are thermally stable and terms involving γ and γ_{m2} can be neglected. In this case Eqs. 11–13 simplify to

$$\frac{dn}{dt} = \frac{A(N-n)}{A(N-n) + A_{m2}m_2 + A_{m1}m_1}X, \tag{15}$$

$$\frac{dm_1}{dt} = \frac{B_1M_1}{B_1M_1 + B_2M_2}X - \frac{A_{m1}m_1}{A(N-n) + A_{m2}m_2 + A_{m1}m_1}X, \tag{16}$$

$$\frac{dm_2}{dt} = \frac{B_2M_2}{B_1M_1 + B_2M_2}X - \frac{A_{m2}m_2}{A(N-n) + A_{m2}m_2 + A_{m1}m_1}X. \tag{17}$$

For our chosen parameters, A_{m1} is large and consequently, from Eq. (16), m_1 rapidly reaches a quasi-steady condition, in which the capture of free holes by m_1 is balanced by recombination with free electrons,

$$\frac{B_1M_1}{B_1M_1 + B_2M_2}X \approx \frac{A_{m1}m_1}{A(N-n) + A_{m2}m_2 + A_{m1}m_1}X. \tag{18}$$

Equation (18) can be solved for m_1,

$$m_1 = \frac{B_1M_1}{B_2M_2}\frac{A(N-n) + A_{m2}m_2}{A_{m1}}. \tag{19}$$

With m_1 small for large A_{m1}, conservation of charge requires

$$n \approx m_2. \tag{20}$$

Combined with Eqs. 19 and 20, Eq. (15) simplifies to

$$\frac{dn}{dt} = \frac{B_2M_2}{B_1M_1 + B_2M_2}\cdot\frac{A(N-n)X}{A(N-n) + A_{m2}n}. \tag{21}$$

This can immediately be integrated to find

$$D = N\frac{B_1M_1}{B_2M_2}\left[\frac{n}{N} - \frac{A_{m2}}{A}\left(\ln\left(1 - \frac{n}{N}\right) + \frac{n}{N}\right)\right], \tag{22}$$

where D is the dose

$$D = \int_0^{t_D} X(t)dt, \tag{23}$$

and where t_D is the exposure time. If X is constant, as in our simulations, then D=X·t_D. Eq. (22) can be inverted to explicitly provide n as a function of dose. For the special case of A=A_{m2}, as used in the simulation, the result simplifies to

$$n_D = N\left[1 - \exp\left(-\frac{B_2 M_2}{B_1 M_1 + B_2 M_2}\frac{D}{N}\right)\right], \tag{24}$$

where the subscript D has been added to n to emphasize that this is the value of n at the end of irradiation at dose D. Equation (24) indicates that n initially grows linearly with dose D at a rate controlled by the ability of m_2 to balance the charge with captured free holes. At higher doses, saturation is approached: $n \to N$.

In summary, at the end of irradiation, n is given by Eq. (24), m_1 is given by Eq. (19), m_2 is given by Eq. (20), and n_c and n_v are given respectively by Eqs. (9) and (10).

5.2. Relaxation at low temperature

After the irradiation stops, $X = 0$ and free electron and free hole populations decay back to zero in the process of relaxation. For relaxation at low temperature such as $T = 100$ K in our simulation, γ and γ_{m2} are both very small. We are interested in how the relaxation process changes the values of n, m_1 and m_2. At the end of irradiation, for the parameters of interest here, we have $n_v << n_c$, $m_2 << n$, m_1 and also $n_c << (N\text{-}n)$. Consequently, n_v is too small to affect n, m_1 or m_2 and can be ignored. n_c is too small to affect n or m_2, but we have to consider its effect on m_1. Under these conditions, the governing equations (1)–(5) reduce to

$$n \approx n_D, \tag{25}$$

$$\frac{dm_1}{dt} = -A_{m1} m_1 n_c, \tag{26}$$

$$m_2 \approx m_{2D} \approx n_D, \tag{27}$$

$$\frac{dn_c}{dt} = -A(N - n_D) n_c - A_{m1} m_1 n_c - A_{m2} m_{2D} n_c. \tag{28}$$

Taking the ratio of Eq. (26) to Eq. (28), we have

$$\frac{dm_1}{dn_c} = \frac{A_{m1} m_1}{A(N - n_D) + A_{m1} m_1 + A_{m2} m_{2D}}. \tag{29}$$

Equation (29) can be immediately integrated to find

$$n_c = n_{cD} + m_1 - m_{1D} + \frac{A(N - n_D) + A_{m2} m_{2D}}{A_{m1}} \ln\left(\frac{m_1}{m_{1D}}\right). \tag{30}$$

Equation (30) provides n_c as a function of m_1. Our interest, however, is in finding m_1 after relaxation when $n_c \approx 0$. To do this, we invert Eq. (30), set $n_c = 0$ and find

$$m_{1,0} = \frac{m_{1D}}{r_D}\Omega\left(\ln(r_D) + r_D\left[1 - \frac{n_{cD}}{m_{1D}}\right]\right), \tag{31}$$

where Ω is the Wright Omega function (see Lawrence et al. (2012)), $m_{1,0}$ is the value of m_1 at the end of relaxation and r_D is the ratio, at the start of relaxation, of the recombination rate of free electrons into m_1 to the sum of the rates of recapture by n and recombination into m_2,

$$r_D = \frac{A_{m1} m_{1D}}{A(N - n_D) + A_{m2} m_2}. \tag{32}$$

Larger values of r_D and n_{cD} lead to a larger drop in m_1 during relaxation.

In sum, the drop in m_1 during relaxation has been computed. m_2 and n remain approximately unchanged from their values at the end of irradiation.

5.3. Heating, first peak

During heating, n becomes thermally unstable before m_2. So, when considering the first peak, we neglect γ_{m2}. Also during heating, $X = 0$. The governing equations 11–13 then reduce to

$$\frac{dn}{dt} = \frac{A_{m2} m_2 + A_{m1} m_1}{A(N - n) + A_{m2} m_2 + A_{m1} m_1} n\gamma, \tag{33}$$

$$\frac{dm_1}{dt} = -\frac{A_{m1} m_1}{A(N - n) + A_{m2} m_2 + A_{m1} m_1} n\gamma, \tag{34}$$

$$\frac{dm_2}{dt} = \frac{A_{m2} m_2}{A(N - n) + A_{m2} m_2 + A_{m1} m_1} n\gamma. \tag{35}$$

Taking the ratio of Eq. (34) to Eq. (35), we find

$$\frac{d\ln(m_1)}{d\ln(m_2)} = \frac{A_{m1}}{A_{m2}}. \tag{36}$$

For the simulation parameters, $A_{m1}/A_{m2} = 5000$. Thus, from Eq. (36), m_1 will empty quickly, long before any significant change happens to m_2. Since at the end of relaxation, $m_1 << n$, no significant change in n will happen during this time either. Under these conditions, Eq. (34) simplifies to

$$\frac{dm_1}{dt} = \frac{A_{m1} n_0}{A(N - n_0) + A_{m2} n_0 + A_{m1} m_1} m_1\gamma, \tag{37}$$

where a subscript 0 is used to indicate the initial value at the beginning of heating and t' is a time integration variable. It follows

$$m_{1,0} - m_1 + \frac{A(N - n_0) + A_{m2} n_0}{A_{m1}} \ln\left(\frac{m_{1,0}}{m_1}\right) = n_0 \int_0^t \gamma(t')dt'. \tag{38}$$

For a linear temperature profile, $T = T_0 + \beta t$, the integral on the right-hand side can be performed analytically to find

$$m_{1,0} - m_1 + \frac{A(N - n_0) + A_{m2} n_0}{A_{m1}} \ln\left(\frac{m_{1,0}}{m_1}\right) = n_0 \frac{Es}{k\beta}[\Gamma(-1, E/kT) - \Gamma(-1, E/kT_0)], \tag{39}$$

where Γ is the incomplete gamma function (see Abramowitz and Stegun (1970)). Equation (39) can be solved for m_1 to find

$$m_1 = \frac{m_{1,0}}{r}\Omega(\ln(r) + ru), \tag{40}$$

where Ω is the Wright Omega function and r and u are abbreviations for

$$r = \frac{A_{m1} m_{1,0}}{A(N - n) + A_{m2} n_0}, \tag{41}$$

$$u = 1 - \frac{n_0}{m_{1,0}}\frac{Es}{k\beta}[\Gamma(-1, E/kT) - \Gamma(-1, E/kT_0)]. \tag{42}$$

Under these conditions, Eq. (9) reduces to

$$n_c = \frac{n_0\gamma}{A(N - n_0) + A_{m1} m_1 + A_{m2} n_0}. \tag{43}$$

The intensity during the first peak is thus

$$I = A_{m1} m_1 n_c, \tag{44}$$

where m_1 is given by Eq. (40) and n_c is given by Eq. (43).

In sum, we have an analytical solution valid for the first peak where m_1 is given by Eq. (40), n_c is given by Eq. (43), and the intensity is given by Eq. (44). The approximate analytical solution is compared with the numerical solution in Fig. 2 (dashed line). The initial conditions for the analytical solution were provided by the relaxation theory in subsection 5.2. For the chosen parameters, the approximation that n and m_2 are nearly constant during the first peak is fairly good and causes only a small overestimate of intensity. The theory remains valid until around $T \approx 160$ K when m_1 drops to a small enough level that the capture of holes freed by thermal excitation, γ_{m2}, from m_2 can no longer be neglected.

5.4. Heating, second peak

While the first peak is occurring, we have $n_c << n$ and the population n_c is quasi-steady as per Eq. (9). As heating continues, the situation reverses. Due to the rapid increase in γ, the trap n empties. We have $n << n_c$ and it is the population n which becomes quasi-steady with the thermal excitation out of n balanced by the capture of free electrons back into n,

$$n\gamma \approx A(N-n)n_c. \tag{45}$$

Or, solving for n,

$$n = \frac{ANn_c}{\gamma + An_c}. \tag{46}$$

Using Eqs. (10) and (45), Eqs. (2)–(4) reduce to

$$\frac{dm_1}{dt} = \frac{B_1M_1}{B_1M_1 + B_2M_2} m_2\gamma_{m2} - A_{m1}m_1n_c, \tag{47}$$

$$\frac{dm_2}{dt} = -\frac{B_1M_1}{B_1M_1 + B_2M_2} m_2\gamma_{m2} - A_{m2}m_2n_c, \tag{48}$$

$$\frac{dn_c}{dt} = -A_{m2}m_2n_v - A_{m1}m_1n_c. \tag{49}$$

At the end of the first peak, the population m_2 was depleted. As γ_{m2} increases and m_2 becomes thermally unstable, some of the holes released from m_2 are captured by m_1. Holes trapped by m_1 quickly recombine with free electrons and the population of m_1 remains small and the holes gained by m_1 due to capture approximately balance the loss of holes due to recombination,

$$\frac{B_1M_1}{B_1M_1 + B_2M_2} m_2\gamma_{m2} \approx A_{m1}m_1n_c. \tag{50}$$

Solving Eq. (50) for m_1 yields

$$m_1 = \frac{B_1M_1}{B_1M_1 + B_2M_2} \frac{m_2\gamma_{m2}}{A_{m1}n_c}. \tag{51}$$

Under these circumstances, we have n, $m_1 << m_2$, n_c. Consequently, by conservation of charge, we must have

$$n_c \approx m_2. \tag{52}$$

Combining Eq. (52), the conservation equation (48) reduces to

$$\frac{dm_2}{dt} = -\frac{B_1M_1}{B_1M_1 + B_2M_2} m_2\gamma_{m2}(t) - A_{m2}{m_2}^2, \tag{53}$$

where the thermal excitation rate is written as $\gamma_{m2}(t)$ to emphasize that, as per Eq. (7), it is a function of temperature and therefore of time. As a first-order ordinary differential equation, solution of Eq. (53) requires one initial condition. We choose this initial condition to be $m_2(t_1) = m_{2,1}$ for some time t_1 and value $m_{2,1}$. The time t_1 can be any time during which the approximations used to develop Eq. (53) are valid. Equation (53) then has the solution

$$m_2 = \frac{m_{2,1} \exp\left(-\frac{B_1M_1}{B_1M_1+B_2M_2} \int_{t_1}^{t} \gamma_{m2}(t')dt' \right)}{1 + A_{m2}m_{2,1} \int_{t_1}^{t} \exp\left(-\frac{B_1M_1}{B_1M_1+B_2M_2} \int_{t_1}^{t'} \gamma_{m2}(t'')dt'' \right) dt'}, \tag{54}$$

where t' and t'' are variables of integration. If we again assume the usual linear temperature profile, $T=T_0+\beta t$, then the integrals over γ_{m2} can be performed analytically,

$$m_2 = \frac{m_{2,1}\{-\alpha[\Gamma(-1, E_{m2}/kT) - \Gamma(-1, E_{m2}/kT_1)]\}}{1 + A_{m2}m_{2,1} \int_{T_1}^{T} \exp\{-\alpha[\Gamma(-1, E_{m2}/kT') - \Gamma(-1, E_{m2}/kT_1)]\} dT'}, \tag{55}$$

where Γ is again the incomplete gamma function and α is an abbreviation for

$$\alpha = \frac{B_1M_1}{B_1M_1 + B_2M_2} \frac{E_{m2}s_{m2}}{k\beta}. \tag{56}$$

The intensity is, as before

$$I = A_{m1}m_1n_c, \tag{57}$$

where m_1 is given by Eq. (51) and n_c is given by the combination of Eqs. (52) and (55).

In sum, we now have a complete solution for the second peak with m_2 given by Eq. (55), n_c given by Eq. (52), n given by Eq. (46), m_1 given by Eq. (51) and the intensity I given by Eq. (57). For the initial condition required by Eq. (55), the value of $m_{2,1}$ was chosen to match the simulation at 220 K. The analytical solution remains accurate over the course of the second peak up until m_1 is no longer small relative to m_2 at which point the quasi-steady approximation Eq. (50) ceases to be valid. The full glow curve reached by using the analytical solutions for the first and second peak and with the mentioned set of parameters is shown in the dashed line of Fig. 2. The close agreement with the simulated results found numerically without approximations as given by the solid line is evident.

5.5. Irradiation at low to mid temperatures

Let us start with the quasi-steady equations 11–13. Since temperatures will be well below 250 K, we can neglect γ_{m2}, yielding

$$\frac{dn}{dt} = \frac{A(N-n)}{A(N-n) + A_{m2}m_2 + A_{m1}m_1} X - \frac{A_{m2}m_2 + A_{m1}m_1}{A(N-n) + A_{m2}m_2 + A_{m1}m_1} n\gamma, \tag{58}$$

$$\frac{dm_1}{dt} = \frac{B_1M_1}{B_1M_1 + B_2M_2} X - \frac{A_{m1}m_1}{A(N-n) + A_{m2}m_2 + A_{m1}m_1} (X + n\gamma), \tag{59}$$

$$\frac{dm_2}{dt} = \frac{B_2M_2}{B_1M_1 + B_2M_2} X - \frac{A_{m2}m_2}{A(N-n) + A_{m2}m_2 + A_{m1}m_1} (X + n\gamma). \tag{60}$$

We will look at the concentrations achieved after irradiation for a long enough time that the concentrations reach a steady-state. To find these concentrations, we set $dn/dt = dm_1/dt = dm_2/dt = 0$ in Eqs. (1)–(3). After some algebra (see appendix), we find n as a function of temperature T,

$$n = N_\gamma(T)\left(\sqrt{1 + 2N/N_\gamma(T)} - 1\right), \tag{61}$$

where N_γ(T) has units of concentration, cm^{-3}, and is an abbreviation for

$$N_\gamma(T) = \frac{B_1M_1/A_{m1} + B_2M_2/A_{m2}}{B_1M_1 + B_2M_2} \frac{AX}{2\gamma(T)}, \tag{62}$$

where the thermal excitation rate γ is written as $\gamma(T)$ to emphasize that it depends on temperature. Similarly, the values of m_1 and m_2 can be found and are proportional to n,

$$m_1 = \frac{B_1M_1/A_{m1}}{B_1M_1/A_{m1} + B_2M_2/A_{m2}} n, \tag{63}$$

$$m_2 = \frac{B_2M_2/A_{m2}}{B_1M_1/A_{m1} + B_2M_2/A_{m2}} n. \tag{64}$$

The rate at which m_1 gains population by trapping holes is proportional to B_1M_1. Note that more precisely, it is $B_1(M_1\text{-}m_1)$, but we assumed that $m_1 << M_1$ so, in our case, $B_1(M_1\text{-}m_1) \approx B_1M_1$. The rate at which m_1 loses population through recombination with electrons is proportional to A_{m1}. It is consequently not surprising that the final population of m_1 in Eq. (63) is proportional to the ratio B_1M_1/A_{m1} and that a similar result holds for m_2.

As temperature increases, γ increases rapidly. Consequently, from Eq. (62), when temperature increases, $N_\gamma(T)$ decreases rapidly and from

Eq. (61), n also decreases rapidly. Without electrons in the trap, thermoluminescence must also decrease. A plot of n from Eq. (61) against irradiation temperature is shown in the solid line of Fig. 4. For the limiting cases of high and low temperature, the limiting values of Eq. (61) are given by.

$n \rightarrow N$ for low temperature: $N_\gamma(T) >> N$,

$$n \rightarrow \sqrt{2NN_\gamma(T)} \text{ for high temperature:} N_\gamma(T) << N. \tag{65}$$

For irradiation temperatures below 130 K, the steady-state trap population is seen to be close to $N = 3 \times 10^9$ cm^{-3}. The trap population n as simulated at 100 K is 2.7 $\times$ 10^9 cm^{-3}, indicating that the simulated results approach within 90% of the steady-state value.

5.6. Relaxation at low to mid temperatures

The equations governing relaxation are the same as Eqs. 58–60 but with $X = 0$,

$$\frac{dn}{dt} = -\frac{A_{m2}m_2 + A_{m1}m_1}{A(N-n) + A_{m2}m_2 + A_{m1}m_1} n\gamma, \tag{66}$$

$$\frac{dm_1}{dt} = -\frac{A_{m1}m_1}{A(N-n) + A_{m2}m_2 + A_{m1}m_1} n\gamma, \tag{67}$$

$$\frac{dm_2}{dt} = -\frac{A_{m2}m_2}{A(N-n) + A_{m2}m_2 + A_{m1}m_1} n\gamma. \tag{68}$$

Since $m_1 << n$ and as per Eq. (67), m_1 is not being replenished, the recombination of electrons with m_1 can only have a minimal effect on n and we can neglect it in Eq. (66). Also, since n_v, n_c, $m_1 \ll n$, m_2, conservation of charge requires $n \approx m_2$. Thus, Eqs. (66) and (68) both reduce to

$$\frac{dn}{dt} = \frac{A_{m2}n^2\gamma}{AN + (A_{m2} - A)n}. \tag{69}$$

Equation (69) can be immediately integrated to find

$$t = \frac{1}{\gamma}\frac{A}{A_{m2}}\left[\frac{N}{n} - \frac{N}{N_D} + \left(\frac{A_{m2}}{A} - 1\right)\ln\left(\frac{n_D}{n}\right)\right], \tag{70}$$

where n_D is the value of the trap concentration at the end of irradiation or the beginning of relaxation. For the special case of $A = A_{m2}$, Eq. (70) can be inverted to find n as a function of time t,

$$n = \frac{n_D}{1 + \frac{n_D}{N}\gamma t}. \tag{71}$$

The trap concentration after a relaxation period of 60 s is shown in the dashed line in Fig. 4. As can be seen in Figs. 3 and 4, the temperature dependence of the simulated TL in Fig. 3 and the trapped electrons

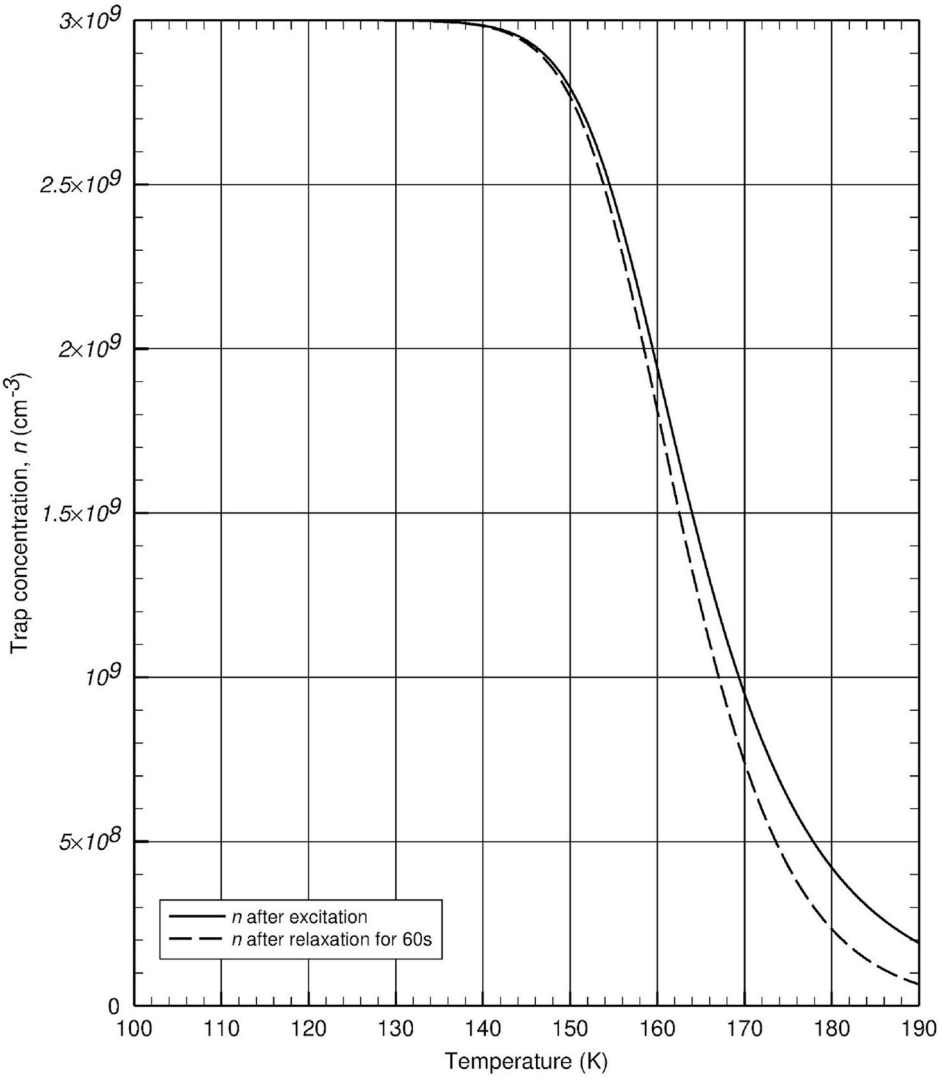

Fig. 4. The concentration of trapped electrons (n) as a function of the temperature of excitation as determined by the theory. The solid line shows the concentration at the end of excitation and the dashed line at the end of 60 s of relaxation.

concentration from Eqs. (61) and (71) have similar appearance for the chosen set of parameters.

6. Discussion

In this work, we use a previously presented energy-level model which can explain the occurrence of temperature ranges below a certain TL peak, in which the sample is not excitable by irradiation that can excite the peak if applied at lower temperature. The motivation is the experimental results in calcium tungstate and semiconducting diamonds published ~50 years ago. In both cases, a glow curve with two peaks at about 150 K and 260 K are excitable when the sample is UV irradiated at LNT or other temperatures below that of the lower peak. However, at temperatures above that of the first peak, the excitation reduced very quickly with increasing temperature so that well below the temperature of the second peak it was not excitable at all. We have considered a model previously used to explain the anomalous heating rate effect. The model includes an electron trap, a hole trap and a hole recombination center. We have written the relevant set of coupled differential equations and for a certain set of trapping parameters, solved the three stages of excitation, relaxation and heating. This was done by simulation consisting of numerical solution of the equations and by a theoretical approximate approach. The results of the two approaches are practically the same, and are rather similar to the mentioned experimental results.

A comment should be made on the parameter ranges for which similar effects may occur. Due to the complex nature of the described process, this can be done only in very general terms. The effect requires two centers and one trap. The first center is thermally stable and has a relatively strong recombination coefficient and the second is thermally unstable and has a weak recombination coefficient. The trap must become thermally unstable at a lower temperature than the second center.

We have also considered the effective trapping parameters of the two simulated peaks. Taking into consideration the complicated process involved, one cannot expect the evaluated parameters to be exactly the same as those inserted into the simulating program. We used for the analysis a peak-shape method based on the evaluation of the peak maximum T_m and the full half-intensity width ω (see e.g., Chen, 1969). The evaluated effective activation energies of the two peaks have been found to be 0.44 eV and 0.54 eV as compared to 0.49 eV and 0.66 eV respectively used in the simulation. The frequency factors have been found to be 7×10^{13} s^{-1} and 9×10^{9} s^{-1} as compared to the inserted values of 5×10^{12} s^{-1} and 3×10^{12} s^{-1} respectively. It is worth noting that the higher-temperature peak looks nearly like a regular first-order peak with the symmetry factor μ_g~0.40. The lower-temperature peak is much more skewed, with μ_g~0.32. This latter value is rather unusual although there are some reports on such experimentally found symmetry factors (see e.g., Tiwari et al., 2014; Tamrakar et al., 2015; Guntu et al., 2020).

It should be noted that in some other experimental cases mentioned in the introduction, in ranges of temperature below that of a certain peak, the TL peak was not excitable. We do not suggest that the present model covers all these cases, but when one encounters such a situation, the possibility of a model like this should be considered. We do not even claim that the parameters we used in the model are directly relevant to calcium tungstate or semiconducting diamonds. It is only suggested that this rather anomalous effect of inability to excite a TL peak at a certain temperature range below that of the peak can sometimes be explained by such a model.

Declaration of competing interest

The authors declare that they have no known competing financial interests or personal relationships that could have appeared to influence the work reported in this paper.

Appendix

We will derive Eqs. (61), (63) and (64). Setting the derivatives in Eqs. 58–60 to zero, we have

$$\frac{A(N-n)}{A(N-n)+A_{m2}m_2+A_{m1}m_1}X=\frac{A_{m2}m_2+A_{m1}m_1}{A(N-n)+A_{m2}m_2+A_{m1}m_1}n\gamma, \tag{A1}$$

$$\frac{B_1M_1}{B_1m_1+B_2M_2}X=\frac{A_{m1}m_1}{A(N-n)+A_{m2}m_2+A_{m1}m_1}(X-n\gamma), \tag{A2}$$

$$\frac{B_2M_2}{B_1m_1+B_2M_2}X=\frac{A_{m2}m_2}{A(N-n)+A_{m2}m_2+A_{m1}m_1}(X-n\gamma). \tag{A3}$$

Taking the ratio of Eq. (A2) to (A3), we have

$$\frac{B_1M_1}{B_2M_2}=\frac{A_{m1}m_1}{A_{m2}m_2}. \tag{A4}$$

Thus,

$$m_1=\frac{B_1M_1}{B_2M_2}\frac{A_{m2}}{A_{m1}}m_2. \tag{A5}$$

From conservation of charge, we know that $n=m_1+m_2$ and thus,

$$n=m_1+m_2=\left(1+\frac{B_1M_1}{B_2M_2}\frac{A_{m2}}{A_{m1}}\right)m_2. \tag{A6}$$

Rearranging (A6), we have

$$m_2=\frac{B_2M_2/A_{m2}}{B_1M_1/A_{m1}+B_2M_2/A_{m2}}n. \tag{A7}$$

Because $n=m_1+m_2$, it immediately follows that

$$m_2=\frac{B_1M_1/A_{m1}}{B_1M_1/A_{m1}+B_2M_2/A_{m2}}n. \tag{A8}$$

Eliminating the common denominator from Eq. (*A1*), we have

$$A(N-n)X = (A_{m2}m_2 + A_{m1}m_1). \tag{A9}$$

Substituting Eqs. (A7) and (A8) into Eq. (A9), we have

$$A(N-n)X = \left(\frac{B_1M_1 + B_2M_2}{B_1M_1/A_{m1} + B_2M_2/A_{m2}}\right)n^2\gamma. \tag{A10}$$

Equation (A10) is quadratic in n and has the solution as given by Eq. (61).

References

Abramowitz, M., Stegun, I.A., 1970. Handbook of Mathematical Functions. US Government Printing Office, Washington, DC.

Chen, R., 1969. Glow curves with general order kinetics. J. Electrochem. Soc. 116, 1254–1257.

Chen, R., Pagonis, V., Lawless, J.L., 2008. Duplicitous thermoluminescence peak associated with thermal release of electrons and holes from trapping states. Radiat. Meas. 43, 162–166.

Chen, R., Pagonis, V., 2017. A model explaining the anomalous heating-rate effect in thermoluminescence as an inverse thermal quenching based on simultaneous thermal release of electrons and holes. Radiat. Meas. 106, 20–25.

Chen, R., Pagonis, V., 2011. Thermally and Optically Stimulated Luminescence: A Simulation Approach. Wiley, Chichester, pp. 92–94.

Durrani, S.A., Groom, P.J., Khazal, K.A.R., McKeever, S.W.S., 1977. The dependence of the thermoluminescence sensitivity upon the temperature of irradiation in quartz. J. Phys. D Appl. Phys. 10, 1351–1361.

Guntu, R.K., Jahangeer, N., Rao, Ch S., 2020. Thermoluminescence, elastic and dielectric investigations of calcium fluoro borophosphate glass composite materials doped by small concentrations of TiO_2. Indian J. Phys. https://doi.org/10.1007/s12648-020-01720-8.

Halperin, A., Chen, R., 1966. Thermoluminescence of semiconducting diamond. Phys. Rev. 148, 839–845.

Halperin, A., 2000. Direct excitation of high temperature thermoluminescence (HTTL) in quartz by low temperature X-irradiation. Nucl. Instrum. Methods Phys. Res. B 166–167, 177–182.

Kitis, G., Charalambous, S., 1988. Thermoluminescence response as a function of irradiation temperature. Nucl. Tracks Radiat. Meas. 14, 91–95.

Kitis, G., Charalambous, S., 1990. Thermoluminescence of high temperature glow peaks of LiF at various irradiation temperatures. Radiat. Protect. Dosim. 33, 259-162.

Klasens, H.A., 1946. Transfer of energy between centres in zinc sulphide phosphors. Nature (London) 158, 306–307.

Kortov, V.S., Milman, I.I., Nikiforov, S.V., 2002. Thermoluminescent and dosimetric properties of anion-defective α-Al_2O_3 single crystals with filled deep trap. Radiat. Protect. Dosim. 100, 75–78.

Lawrence, P.W., Corless, M.L., Jeffrey, D.J., 2012. Algorithm 917: complex double-precision evaluation of the Wright Ω function. ACM Trans. Math Software 38. Article #20.

Mikhailik, V.B., Kraus, H., Wahl, D., Itoh, M., Koike, M., Bailiff, I.K., 2004. One- and two-photon excited luminescence and band-gap assignment in $CaWO_4$. Phys. Rev. B69, 1–9, 205110.

Molnár, G., Benabdelsselam, M., Borossay, J., Lapraz, D., Iacconi, P., Akselrod, M., 2001. Influence of the irradiation temperature on TL sensitivity of Al_2O_3. C. Radiat. Meas. 33, 619–623.

Nikiforov, S.V., Milman, I.I., Kortov, V.S., 2001. Thermal and optical ionization of F-centers in the luminescence mechanism of anion-defective corundum crystals. Radiat. Meas. 33, 547–551.

Sayer, M., Souder, A.D., 1967. Impurities and trappimg states in calcium tungstate. Phys. Lett. 24A, 246–247.

Sayer, M., Souder, A.D., 1969. On the origin of defect states in calcium tungstate. Can. J. Phys. 47, 463–471.

Sayer, M., Lynch, G.F., 1970. Ultra-violet excited paramagnetic centres in calcium tungstate. Phys. Status Solidi 37, 673–681.

Schön, M., 1942. Zum leuchtmechanismus der Kristallphosphore. Z. Phys. 119, 463–472.

Tamrakar, R.K., Tiwari, N., Kuraria, R.K., Bisen, D.P., Dubey, V., Upadhyay, K., 2015. Effect of annealing temperature on thermoluminescence glow curve for UV and gamma ray induced ZrO_2:Ti phosphor. J. Radiat. Res. Appl. Sci. 8, 1–10.

Tiwari, N., Kuraria, R.K., Tamrakar, R.K., 2014. Thermoluminescence glow curve for UV induced ZrO_2:Ti phosphor with variable concentration and various heating rate. J. Radiat. Res. Appl. Sci. 7, 542–549.

Winer, S.A.A., Kristianpoller, N., Chen, R., 1973. In: Williams, Ferd (Ed.), Effects of Thermoluminescence Excitation in Semiconducting Diamonds. Luminescence of Crystals, Molecules and Solutions. Plenum Pub. Corp., pp. 473–477